

Magnetic properties of various crystalline phases and amorphous Al-Si-Mn and Al-Mn alloys

J. J. Hauser, H. S. Chen, G. P. Espinosa, and J. V. Waszczak

AT&T Bell Laboratories, Murray Hill, New Jersey 07974

(Received 8 May 1986)

The present study examines the magnetic properties of four distinct magnetic systems. First, the range of amorphous Al-Mn films was extended down to 7.5 at. % Mn from the previous limit of 14 at. % obtained on both amorphous films and icosahedral ribbons, such films still exhibiting a local magnetic moment ($\approx 0.54\mu_B$). Second, quenched supersaturated fcc Al-Mn alloys in the form of film and melt-spun ribbons display a local magnetic moment similar to that observed in amorphous and icosahedral phases. Third, the α -Al₇₃Si₁₀Mn₁₇ phase, similarly to orthorhombic Al₆Mn, does not exhibit a local magnetic moment. Finally, the ferromagnetism discovered in amorphous Al-Si-Mn melt-spun ribbons has now been observed in crystalline alloys with a structure similar to β -Al-Mn-Si.

I. INTRODUCTION

The magnetic properties of Al-Si-Mn and Al-Mn quasicrystals and amorphous films were recently reported.¹ The most important result of this study was the existence of a local magnetic moment in the quasicrystalline phase of Al₈₆Mn₁₄ which disappears after annealing into the crystalline orthorhombic phase. Furthermore, the effective local magnetic moment increases with Mn content up to $(1.5 \pm 0.5)\mu_B$ in both Al-Mn and Al-Si-Mn alloys. A more recent investigation² by the NMR spin-echo technique has established that there is a distribution of both magnetic and nonmagnetic Mn sites. At low Si content (≤ 6 at. %) the magnetic properties of the amorphous and icosahedral phases are similar^{1,3,4} and the moments seem to order in a spin-glass state.¹ At high Si levels (e.g., Al₃₆Si₄₀Mn₂₄) ferromagnetism prevails but the source of ferromagnetism remains unidentified.

Since single-phase icosahedral samples cannot be prepared⁵ with less than 14 at. % Mn and since the icosahedral and amorphous phases are magnetically similar,¹ one of the goals of the present study is to extend the magnetic measurements to amorphous alloys with less than 14 at. % Mn. On the other hand, it has been known and ignored for a long time that Al can dissolve considerably larger amounts of Mn than the equilibrium if melts are rapidly water or air quenched.⁶ The supersaturation as indicated by lattice-parameter measurements can be as high as 4.7 at. % or 6.7 times higher than the maximum equilibrium solubility (0.7 at. %). However, the magnetic properties of such crystalline supersaturated alloys are unknown and will be examined in the present study. It has also been suggested both theoretically⁷ and by recent extended x-ray absorption fine-structure (EXAFS) measurements^{8,9} that the structure of the icosahedral phase is similar to that of the α -Al-Mn-Si phase. We will examine this suggestion by measuring the magnetic properties of the α phase. Finally, the present study will be concluded by an attempt to explain the source of the ferromagnetism discovered¹ in amorphous Al-Si-Mn ribbons with high Si contents.

II. EXPERIMENTAL PROCEDURE

The Al-Mn films were sputtered at 260 K onto Mylar (polyethylene terephthalate) and the supersaturated Al-Mn alloy ribbons were prepared by melt spinning. The magnetic susceptibility of films and ribbons was measured in a low-field (4 Oe) ac susceptibility apparatus at 10 kHz and in a high-field (10.6 kOe) susceptibility apparatus using the Faraday method. The ferromagnetic Al-Mn and Al-Si-Mn alloys were prepared following Kono's original work¹⁰ by inductively melting in alumina crucibles the desired proportions of electrolytic manganese (99.9% pure) and aluminum (99.99% pure). These melts were then crushed and remelted in a glow-bar furnace and cooled from the melt to 600°C in approximately 1 min. The structure of all the samples was determined by x-ray diffraction.

III. EXPERIMENTAL RESULTS AND DISCUSSION

The magnetic properties of Al-Mn films and ribbons are summarized in Table I. Starting with the films and using the similarity¹ between amorphous films and icosahedral ribbons, one would expect based on the plot of the local magnetic moment per Mn atom, p_{eff} , versus manganese concentration C_{Mn} (Fig. 3 of Ref. 1) that amorphous alloys with 10 and 7.5 at. % Mn should be characterized by p_{eff} values of, respectively, $0.25\mu_B$ and $0.14\mu_B$. These values are appreciably smaller than those shown in Table I, and a further inconsistency is shown by the fact that the 7.5 at. % Mn film has a larger p_{eff} value than the 10 at. % Mn film. Since a crystalline 5 at. % Mn film displays a fairly large magnetic moment of $1.55\mu_B$, one may think that these discrepancies are caused by the presence of some microcrystallinity. The amount of microcrystallinity must be very small since the diffraction pattern shown in Fig. 1 for the 7.5 at. % Mn (which is identical to that for the 10 at. % Mn film) is typical of a truly amorphous film: the rounded maximum centered at $2\theta \approx 43^\circ$ occurs where the strongest diffraction peaks of both orthorhombic and icosahedral Al₆Mn are situated

TABLE I. Magnetic properties of amorphous and crystalline Al-Mn alloys.

Sample	Type	Structure	p_{eff} units of (μ_B)	$-\Theta$ (K)	$10^6\chi_0$ (emu g $^{-1}$)	$10^6\chi_{4.2\text{ K}}$ (emu g $^{-1}$)	$10^6\chi_{300\text{ K}}$ (emu g $^{-1}$)
Al ₉₀ Mn ₁₀	film	amorphous	0.46	2	0.39	13.3	0.7
Al _{92.5} Mn _{7.5}	film	amorphous	0.63	11	2.5	14.8	2.8
Al ₉₅ Mn ₅	film	crystalline	1.55	3	1.76	55	3.5
Al _{92.5} Mn _{7.5}	ribbon	crystalline	0.97	15	2.34	25.2	3.3
Al ₉₅ Mn ₅	ribbon	crystalline	1.06	22	2.61	18	3.4
Al _{97.5} Mn _{2.5}	ribbon	crystalline	0			5.3	2.3

and there is a complete absence of intensity in the regions of the (111) and (200) Al diffraction peaks which appear very strongly when C_{Mn} is reduced to 5 at. %. This result is remarkable in itself since Mn is not a glass former such as P or Si, and it is therefore surprising, that such a small amount of Mn (7.5 at. %) stabilizes a thick amorphous film deposited at essentially room temperature. Anyhow, the p_{eff} values for the 10 and 7.5 at. % Mn amorphous films can be rationalized by assuming that they contain, respectively, 6.6 and 12.1 wt. % of crystalline Al₉₅Mn₅ clusters. Such a small amount of microcrystallinity could indeed be missed in the x-ray diffraction and is consistent with the appearance of crystallinity at 5 at. % Mn. The existence of a magnetic moment in these amorphous alloys is consistent with a recent NMR spin-echo study² which concluded that in Al_{1-x}Mn_x icosahedral ribbons there is a constantly rising fraction of magnetic sites in the range $0.14 \leq x \leq 0.22$. Furthermore, the estimate of the nonmagnetic mole fraction x_{NM} was obtained on icosahedral ribbons and despite the approximate similarity previously mentioned between the amorphous and

icosahedral phases, one would expect amorphous films to have a larger magnetic moment because of their large inherent disorder. The relationship between magnetic moment and disorder will be further discussed with the magnetic properties of the α phase. Although these amorphous films display a local magnetic moment, the Curie-Weiss law [$\chi = \chi_0 = C/(T - \Theta)$] is obeyed down to 1.5 K; the absence of spin-glass interaction is consistent with its disappearance¹ in the icosahedral and amorphous phases for $x \leq 0.16$.

We shall now turn our attention to supersaturated fcc Al-Mn ribbons and films. One difference between the two modes of preparation is revealed in the 7.5 at. % Mn alloy: the ribbon is crystalline while the film is amorphous, undoubtedly as a result of the faster quenching rate of the latter. On the other hand, there is no appreciable difference between the two modes of preparation when both samples are crystalline as shown in Fig. 2 which displays the variation of the lattice parameter with C_{Mn} . As

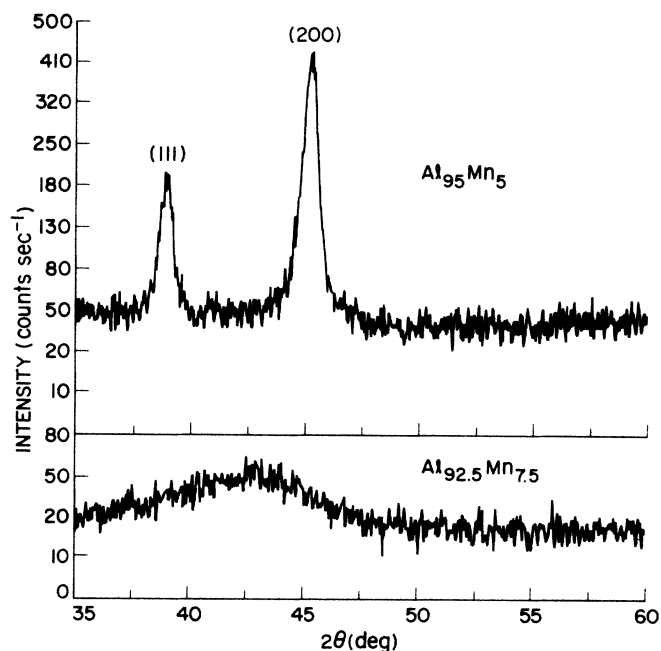


FIG. 1. X-ray diffractometer traces taken with Cu $K\alpha$ radiation: top, 9.8 μm thick Al₉₅Mn₅ film deposited at 260 K; bottom, 10.4 μm thick Al_{92.5}Mn_{7.5} film deposited at 260 K.

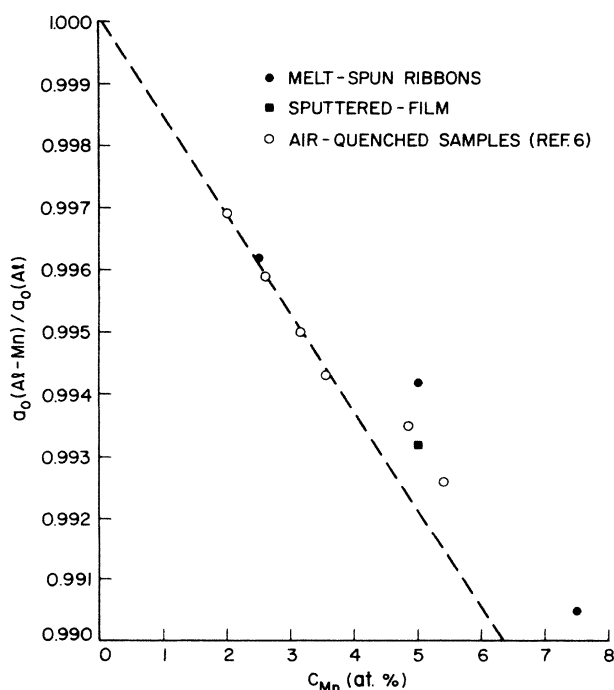


FIG. 2. Ratio of the lattice parameter of the Al-Mn alloy to the lattice parameter of pure Al as a function of Mn concentration.

shown in Fig. 2 the data obtained on ribbons and on a sputtered film are in good agreement with those previously obtained on air-quenched samples.⁶ We observe similar deviations from the dashed line at higher C_{Mn} which were attributed⁶ to a phase separation which was actually observed in the x-ray diffraction pattern of the 7.5 at. % Mn sample. As summarized in Table I, one finds that for $C_{Mn} \geq 5$ at. % both ribbons and films display a local magnetic moment while the ribbon with 2.5 at. % Mn has no local magnetic moment. This latter result is in agreement with the magnetic state of equilibrium solid solutions ($C_{Mn} \leq 0.32$ at. %) where it is known that Mn has a non-magnetic localized d state.^{11,12} The appearance of the local magnetic moment for $C_{Mn} > 2.5$ at. % can be explained with a similar rationale to that used for the increase in p_{eff} with C_{Mn} in icosahedral ribbons:¹ the local moment arises as a result of a pair interaction between Mn localized d -wave functions. On the other hand, since as in icosahedral ribbons² not all Mn sites may be magnetic and the number of magnetic sites may increase with increasing C_{Mn} , the data shown in Fig. 2 could be interpreted by assuming that the local moments are carried by Mn atoms which are not in the ordered fcc lattice. Indeed, the 2.5 at. % Mn alloy, in which essentially all the Mn is in solid solution, displays no moment and the moment appears for $C_{Mn} \geq 5$ at. % where a small amount of Mn is precipitated out on such defects as grain boundaries. At any rate, whatever the microscopic differences may be, the magnitude of p_{eff} is essentially the same in the three phases (fcc, amorphous, and icosahedral) and it most probably has a common origin: disorder.

The close structural relationship⁷ between the icosahedral and α phases of Al-Mn-Si suggests measuring the magnetic properties of the α phase: they are displayed in Fig. 3. Consequently, contrary to the structural similarity, the magnetic properties of the icosahedral and α phases are dissimilar since the latter has no local magnetic

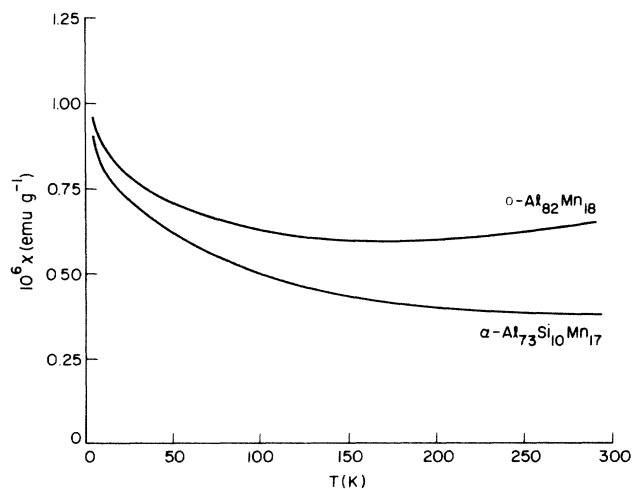


FIG. 3. Temperature dependence of the high-field (10.6 kOe) susceptibility of orthorhombic (o)Al₈₂Mn₁₈ obtained by crystallizing the icosahedral ribbon and of bulk polycrystalline α -Al₇₃Si₁₀Mn₁₇.

moment. Indeed, as shown in Fig. 3, the magnetic properties of the α phase are quite similar to those of the orthorhombic phase with approximately the same Mn content which in turn are similar to those shown in Fig. 1 of Ref. 1 for o-Al₈₆Mn₁₄ (one should note that the χ scale in that figure is 100 times larger than that used in Fig. 3 of the present study). The discrepancy between structure and magnetic properties can be elucidated by some recent EXAFS measurements⁸ which argue that while the α phase is simply a bcc packing of Mackay icosahedra,⁷ the connections between icosahedra are more disordered in the icosahedral phase. One could therefore speculate that the magnetic Mn sites are located in these disordered connection regions. Consequently, the magnetic moment observed in fcc supersaturated solutions and in the icosahedral and amorphous phases is the result of disorder. This is why the moment is absent in the fully ordered α and orthorhombic structures. As previously mentioned, one would expect the amorphous phase, which is the most disordered as a result of the largest quenching rate, to exhibit the greatest number of magnetic sites.

This study will now be completed by an analysis of the ferromagnetism previously discovered¹ in amorphous Al₃₆Si₄₀Mn₂₄ ribbons. A possible source for the ferromagnetism was thought to be a Heusler alloy composition of the type Cu₂MnAl, however the corresponding amorphous alloy Al₂₅Si₅₀Mn₂₅ was only weakly ferromagnetic (Curie temperature $T_C = 12$ K) ruling out such an explanation. Another possibility may be the metastable tetragonal phase Al₅₀Mn₅₀ discovered by Kono.¹⁰ The ferromagnetic phase can only be obtained by air cooling the hexagonal h phase¹⁰ from 950°C. Indeed, if one either

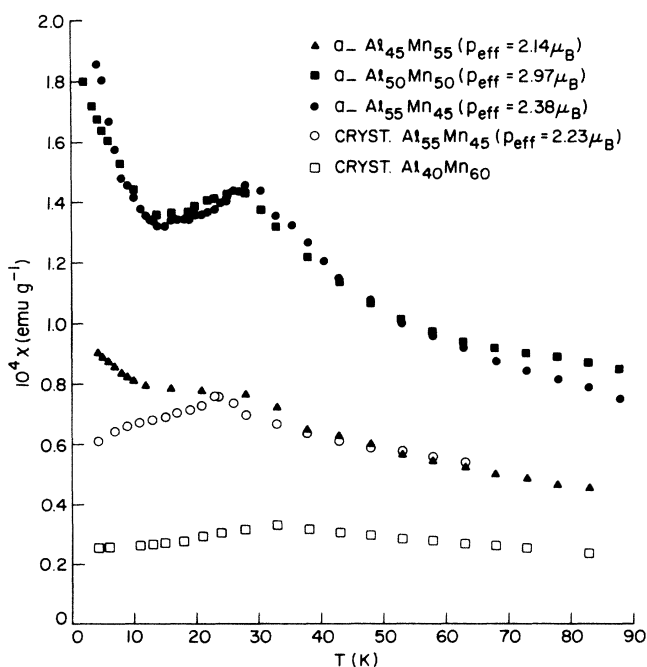


FIG. 4. Temperature dependence of the ac susceptibility of various Al-Mn alloys with compositions close to those of ferromagnetic samples.

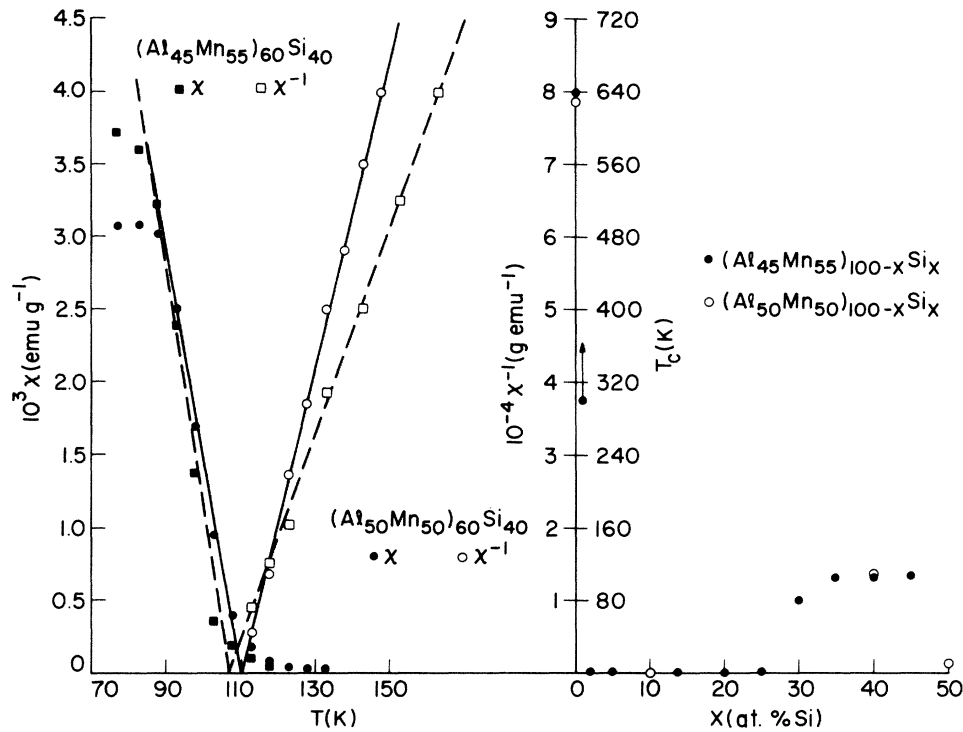


FIG. 5. Left: temperature dependence of the susceptibility and inverse susceptibility for $Al_{27}Mn_{33}Si_{40}$ and $Al_{30}Mn_{30}Si_{40}$ near the Curie temperature ≈ 110 K. Right: dependence of the Curie temperature on Si content for the two ferromagnetic compositions $Al_{45}Mn_{55}$ and $Al_{50}Mn_{50}$.

quenches the h phase or allows the h phase to transform to the equilibrium ζ and β hexagonal phases,¹⁰ the resulting sample is nonferromagnetic at room temperature. The tetragonal phase has a Curie point of 643–653 K; the magnetic moments per Mn atom (p_{eff}) estimated from the low-temperature saturation magnetization and a Curie-Weiss fit of the susceptibility were $2.18\mu_B$ and $3.17\mu_B$, respectively. In agreement with Kono's study we found that $Al_{45}Mn_{55}$ and $Al_{50}Mn_{50}$ with the tetragonal structure are ferromagnetic with T_C 's of 640 and 630 K, respectively. Furthermore, similar cooling of $Al_{55}Mn_{45}$ and of $Al_{40}Mn_{60}$ yields, respectively, the ζ and β phases which are nonferromagnetic; as suggested by the susceptibility maxima of Fig. 4 these alloys would seem to order in a spin-glass state. On the other hand, sputtering at room temperature the ferromagnetic compositions (50 and 55 at. % Mn) produces nonferromagnetic amorphous films which again seem to order in a spin-glass state (Fig. 4). This result is not surprising since one expects a film deposition to yield similar results to the quenching of the high-temperature h phase. In the amorphous state, the spin-glass properties are quite similar whether the composition is in the ferromagnetic range (50 at. % Mn) or not (e.g., 45 at. % Mn). A small amount of ferromagnetism could be responsible for the increase in χ below 15 K shown by amorphous films (Fig. 4). It is also interesting that the p_{eff} values for the spin-glass samples described in Fig. 4 are similar to those reported for the ferromagnetic samples.

At this point one may question whether the magnetic properties of these Al-Mn alloys provide a clue to the

understanding of the ferromagnetism of amorphous $Al_{36}Si_{40}Mn_{24}$ ribbons. An obvious approach is to choose the optimum ferromagnetic binary alloy and study the dependence of T_C on Si. This is shown in the right-hand side of Fig. 5 and it is obvious that the metastable tetragonal phase is not the proper explanation since the ferromagnetism disappears completely upon the addition of a few at. % of Si. However, ferromagnetism reappears for $Si \geq 30$ at. % and is strongest for $Si \approx 40$ at. %. Although the structure of these samples could not be unambiguously identified, it seems closely related to that of β -Al-Mn-Si. One notices again that ferromagnetism disappears close to the Heusler composition (50 at. % Si); as a matter of fact, the T_C for this crystalline alloy (12 K) is the same as that reported for the corresponding amorphous ribbon.¹ The ferromagnetic transition for the optimum composition shown in the left-hand side of Fig. 5 is quite similar to that reported in Fig. 4 of Ref. 1 for the amorphous $Al_{36}Si_{40}Mn_{24}$ except for the magnitudes of the susceptibilities. Indeed, the susceptibility of the crystalline alloy is almost an order of magnitude larger than that of the amorphous ribbon. Linking this result with the fact that ferromagnetism almost disappears in an amorphous $Al_{36}Si_{40}Mn_{24}$ film¹ would suggest that the ferromagnetism observed in the ribbons may arise from clusters with a structure similar to the β -Al-Mn-Si phase.

IV. CONCLUSIONS

The local magnetic moment previously discovered in amorphous and icosahedral phases for $Mn \geq 14$ at. % per-

sists in the amorphous phase for $Mn \geq 7.5$ at. %. A local moment was also observed in fcc supersaturated Al-Mn alloys for $Mn \geq 5$ at. %. On the other hand, similar to the orthorhombic phase, the α phase does not possess a magnetic moment. These results suggest that the magnetic moment is a consequence of structural disorder. Finally, the ferromagnetism observed in amorphous $Al_{36}Si_{40}Mn_{24}$

ribbons may arise from a short-range order similar to the β -Al-Mn-Si structure.

ACKNOWLEDGMENT

We would like to thank R. J. Felder for his technical assistance.

¹J. J. Hauser, H. S. Chen, and J. V. Waszczak, *Phys. Rev. B* **33**, 3577 (1986).

²W. W. Warren, H. S. Chen, and G. P. Espinosa (unpublished).

³W. W. Warren, H. S. Chen, and J. J. Hauser, *Phys. Rev. B* **32**, 7614 (1985).

⁴M. Eibschutz, H. S. Chen, and J. J. Hauser, *Phys. Rev. Lett.* **56**, 169 (1986).

⁵D. Schechtman and I. Blech, *Metall. Trans.* **16A**, 1005 (1985).

⁶G. Falkenhagen and W. Hofman, *Z. Metallkde.* **43**, 69 (1952).

⁷V. Elser and C. L. Henley, *Phys. Rev. Lett.* **55**, 2883 (1985).

⁸Y. Ma, E. A. Stern, and C. E. Bouldin (unpublished).

⁹M. A. Marcus, H. S. Chen, G. P. Espinosa, and C. L. Tsai, *Solid State Commun.* **58**, 227 (1986).

¹⁰H. Kono, *J. Phys. Soc. Jpn.* **13**, 1444 (1958).

¹¹A. B. Kaiser, *J. Phys. C* **3**, 409 (1970).

¹²J. J. Hauser, *Phys. Rev. B* **5**, 1830 (1972).